Clinicopathological progression and molecular characterization of intestinal dilatation syndrome in commercial brown layers

Álex Gómez[1,2*], Ana Rodríguez-Largo[1], Estela Pérez[1,2], Serafín García Freire[3], Christiane Hundehege[4], Eva Berberich[4], Lluís Luján[1,2], Diego Cortés[1,5]

[1]Departamento de Patología Animal, Universidad de Zaragoza, Zaragoza, Spain.

[2]Instituto Agroalimentario de Aragón-IA2, Universidad de Zaragoza, Zaragoza, Spain.

[3] Boehringer Ingelheim España, Sant Cugat del Vallès, Barcelona, Spain.

[4]SAN Group Biotech Germany GmbH, Muehlenstraße, Germany.

[5]Ibérica de Tecnología Avícola, IBERTEC S.A.U., Valladolid, Spain.

***Correspondence:**

Álex Gómez

Departamento de Patología Animal

177 Miguel Servet Street

50013 Zaragoza, Spain

a.gomez@unizar.es

Abstract

Intestinal dilatation syndrome (IDS) is a poorly described condition affecting layers and breeder hens globally. Its prevalence is increasing, particularly in free-range systems, but the etiology remains unknown. This retrospective study examined 35 hens from three flocks: free-range flock A (n=20) and enriched-caged flock B (n=5), both affected by IDS, and enriched-caged flock C (n=10), with no history of IDS. Clinicopathological studies were performed on these hens, and metagenomic analysis was conducted on the proventriculus and jejunum of hens from flock A (n=2) and flock C (n=2). Based on clinical signs and lesions, three progressive stages of IDS were identified. In the first stage, although hens were without clinical signs, proventricular dilatation, lymphoplasmacytic and heterophilic jejunitis and duodenitis were observed. The second stage was marked by cachexia, pale and small combs and wattles, and severe egg production drop. Jejunal dilatation was observed, with microscopic evidence of necrotic, lymphoplasmacytic and heterophilic jejunitis; ganglioneuritis; and mineralization of the jejunal nervous plexuses and subserosal ganglia. In the third stage, spontaneous death occurred due to jejunal volvulus and vascular involvement. Affected hens (stage 2) also exhibited elevated cloacal temperatures (>0.9ºC) and marked heterophilia. Metagenomic analysis identified sequences consistent with *Megrivirus C* in IDS-affected hens and a disruption of the gut microbiota, with increased abundance of *Fusobacterium mortiferum* and *Megamonas funiformis*. In conclusion, this study describes in detail the clinicopathological progression of the IDS and suggests that *Megrivirus C*, in combination with opportunistic intestinal bacteria, could play a role in the pathogenesis of this disease.

Keywords: enteritis, intestinal dilatation syndrome, layers, *Megrivirus*, metagenomic analysis

Intestinal dilatation syndrome (IDS) is an under-characterized condition affecting layer and breeder hens, particularly in cage-free systems. [22,30,33] IDS predominantly impacts females white and brown laying breeders and commercial hens, typically between 30 and 60 weeks of age, during mid-laying, [22,33] but recurring outbreaks often affect younger birds. [33] Since its first description in 2004, [30] reports of IDS have increased globally. [22,25,33] IDS is a progressive disease leading to significant economic losses, marked by irreversible declines in egg production, water and feed intake, breast weight, and increase culling rates. [25,30,33] While the morbidity of IDS remains unknown, mortality rates vary between 5-20%. [22,30,33]

Affected hens exhibit lethargy; dehydration; loss of body condition; and pale combs, beaks, legs, claws, and oral-ocular mucosa due to anemia. [22,33] Diarrhea is an inconsistent finding. [22,30,33] Spontaneous deaths have been linked to septicemia of intestinal origin. [30] The primary gross lesions are found in the jejunum, characterized by pronounced dilatation, affecting the proximal segment to Meckel´s diverticulum. [22,33] The mesenteric blood vessels supplying the dilated jejunal are conspicuous and ectatic. [33] In some cases, the jejunum is twisted, intussuscepted, and infarcted. [33] The duodenum often shows moderate thickening of the intestinal wall. [22,33] Histopathological findings in IDS include lymphoplasmacytic and heterophilic jejunitis, which progresses to atrophic and ulcerative jejunitis. [22,30,33] Additionally, lymphoplasmacytic duodenitis and ileitis, serositis of affected small intestine sections, lymphoplasmacytic and heterophilic perineuritis of the jejunal submucosal and myenteric plexuses, and atrophic lymphoplasmacytic pancreatitis have been associated with IDS. [22,30,33] Perineuritis likely results from severe necrotic-ulcerative jejunitis and is suggested as a probable cause of the jejunal dilatation and intestinal stasis. [22]

The etiology of IDS remains unclear, though finely ground feed, early pathogen or allergen exposure during the rearing period, and genetic predisposition have been suggested as potential contributing factors. [30,33] Recently, chicken parvovirus (ChPV) and megrivirus have been linked to this syndrome. ChPV DNA has been detected in the intestines, pancreas, and proventriculus in IDS-affected hens via PCR assays. [22] However, the reproduction of enteric lesions similar to those observed under natural conditions has not been confirmed experimentally with ChPV. [23] Moreover, ChPV has been associated with other non-IDS correlated diseases, including runting-stunting syndrome, acute catarrhal enteritis, curving of duodenal loop, mesenteritis, pancreatitis, and pancreatic atrophy in young broilers. [11,23] Megrivirus has been detected in animals with enteric diseases. [3,5,12,13,15] However, it has also been found in the intestines of healthy chickens. [16,17] Therefore, the role of megrivirus in avian intestinal pathology remains uncertain. Further research is needed to confirm ChPV or megrivirus as the causative agent of IDS.

This study aimed to characterize the clinicopathological progression and stages of IDS in commercial brown layers. Viral and bacteriological metagenomic analyses were conducted to explore potential etiological associations.

Materials and Methods

Animals and Clinicopathological Studies

A retrospective study was performed with the following data kindly provided by IBERTEC S.A.U. Field cases of IDS were observed in commercial brown layers (40 to 60-weeks-old) from northeastern Spain in 2024, managed under two different systems: free-range (flock A) and enriched cages (flock B). Both flocks originated from the same rearing farm, though not from the same housing unit. For the study, 25 hens from flock A (n=20) and flock B (n=5) were randomly selected. Additionally, a third enriched-cage

flock, originated from other rearing farm (flock C), with no history of IDS, was used to select randomly 10 hens as negative controls. At day 0 (T0), four affected hens from flock A, two affected hens from flock B, and five healthy hens from flock C were sampled. Three to five weeks later (T1), an additional 10 affected hens from flock A, three affected hens from flock B, and five healthy hens from flock C were sampled. Finally, two to three weeks after the second sampling (T2), six affected hens from flock A were sampled. From flock A (n=10) and flock C (n=10), 20 hens were randomly selected for cloacal temperature measurement at T1, with an electronic thermometer on the farm. Whole blood samples from flock A (n=5) and flock C (n=5) were collected at T1 into EDTA-anticoagulant tubes for hematological analysis. Hematocrit (L/L; reference interval (RI): 0.3-0.4), hemoglobin (g/L; RI: 70-186), thrombocytes (g/L; RI: 10-40), and leukocytes (g/L; RI: 12-30) were quantified using an IDEXX ProcyteDx automatic hematology counter (IDEXX laboratories, Westbrook, ME, USA). A manual blood smear was performed to estimate and differentiate leukocyte types: heterophils (%; RI: 20-50), lymphocytes (%; RI: 30-60), monocytes (%; RI: 1-8), eosinophils (%; RI: 1-3), and basophils (%; RI: 1-3). Absolute counts (g/L) of these cell types were also recorded; however, RI are not established for this species. Hypochromia and anisocytosis were also evaluated in the blood smears.

Animals were humanely euthanized on the farm. A complete postmortem examination was conducted on all animals. Samples of the ventriculus, proventriculus, duodenum, jejunum, ileum, colon, cecal tonsil, bursa of Fabricius, and pancreas were collected and fixed in 10% neutral-buffered and sent to the University of Zaragoza for the paraffin embedding. Four-micrometer thick sections were stained with hematoxylin and eosin for the histopathological analysis.

Hens were classified into different stages of IDS based on clinical signs and macroscopic and microscopic findings. These stages represented sequential phases of the disease.

Molecular Detection

For metagenomic analysis, two animals from flock A (A1 and A2) affected by IDS, and two healthy animals from flock C (negative controls, C1 and C2) were selected at T1. Samples from the proventriculus and jejunum were obtained using sterile materials; intestinal contents were removed with sterile physiological saline solution and the mucosa from both organs was impregnated on FTA classic cards (Whatman plc, Maidstone, United Kingdom). The proventriculus and jejunum samples from each animal were pooled. Metagenomic analysis was performed by BASE$_2$BIO LLC (Oshkosh, WI, USA).

Total DNA and RNA were extracted from pooled 3x FTA-cards and 1x GenSaverCard using the Kylt RNA / DNA Purification Kit (SAN Group Biotech Germany, Höltinghausen, Germany) following the manufacturer's guidelines. The kit employs a spin column design and a silica membrane-based purification; the protocol consists of a lysis- and binding-step, followed by two wash steps and an elution step. To reduce unwanted sequencing reads, an in-house protocol was implemented to deplete host rRNA by using complementary DNA probes, followed by RNase H digestion. For untargeted metagenomic sequencing libraries were generated using the Watchmaker RNA-Library Prep Kit (Watchmaker Genomics, Boulder, CO, USA) according to the provided instructions. The library prep workflow consists of RNA fragmentation, first strand cDNA synthesis using reverse transcriptase, and second strand cDNA synthesis, followed by adapter ligation and library amplification. The final pooled library was sequenced on an Illumina MiSeq platform (Illumina, San Diego, CA, USA) with the MiSeq Reagent Kit v2 (300-cycles). Data analysis and interpretation were carried out by

Base2Bio (Oshkosh, WI, USA) using their next-generation sequencing untargeted "discovery" pipeline (avian) (version 0.054).

The data were represented in families, genera, and species and described in read counts and abundance (%). Read counts referred to the frequency of which a specific nucleotide sequence (or fragment) is sequenced or detected. Each read represented a short segment of DNA or RNA generated during the sequencing process. Read counts were essential for understanding the relative abundance of sequences within the overall dataset. Some reads could only be classified at higher taxonomic levels due to their origin from conserved regions shared among multiple lower-level taxa. Consequently, estimating relative abundance based solely on specific read counts may yield highly inaccurate results. To mitigate this issue, an estimated read count was calculated for each node at every taxonomic level. This count encompassed not only specific reads for that node or its descendants but also apportioned reads from parent nodes. Parent node reads were distributed to descendants based on the proportional specific read counts of each, and this process was applied throughout the taxonomic hierarchy. These adjusted counts aimed to represent the "true" read counts for each taxon, typically offering a more accurate quantitative estimate than relying solely on specific reads. However, these estimates did not account for variations in sequence "uniqueness" within the search database, which may introduce additional inaccuracies. The estimated abundances represented the fraction of all classified reads rather than an exact count of genomes or organisms, as they do not consider genome size. Furthermore, given the absence of internal standards for normalization, these relative values were contingent upon the abundance of other taxa present. Final taxonomic classifications were filtered based on a modelled probability, presented at different confidence levels: stringent, relaxed, and occasionally unfiltered. In this study, stringent and relaxed cutoffs were set at 0.8 and 0.4, respectively. For

borderline taxa (determined by k-mer count thresholds and maximum read counts), further analysis was conducted. Reads assigned to these taxa were reanalyzed using BLASTN against the nucleotide (nt) database. Each read was reassigned to the lowest common ancestor based on the top BLAST matches. A b-score was then calculated, representing the proportion of originally assigned reads that were confirmed at that node or lower by BLAST. Additional stringent and relaxed thresholds of 10^{-4} were applied to these taxa before they were reported.

Statistical Analysis

Data were analyzed using IBM SPSS 26.0 for Windows. Continuous variables (cloacal temperatures and hematology results) were represented as mean and standard deviation (±SD). After testing normal distribution of the data by Shapiro–Wilk test, Levene's test was used to evaluate homogeneity of variance for normally distributed variables. For normally distributed variables with equal variances, the Student's T-test was applied. For normally distributed variables with unequal variances, Welch's t-test was applied. For non-normally distributed variables, the Mann–Whitney U test was conducted. The significance level (α-error) was set at 0.05.

Results

Clinical Examination

The progression of IDS was divided into 3 stages (**Table 1**). Animals from flocks A and B were found in different stages of the disease (**Table 2**). In the first stage (T0), affected animals presented without clinical signs. During the second stage (T1), hens exhibited signs of apathy, depression, ruffled feathers, and poor body condition. The beaks, legs, claws, combs and the oral and ocular mucosa were pale (**Supplemental**

Figure S1). Affected animals showed a significant decrease in egg production. In the third stage (T2), animals died spontaneously.

At T1, flock A exhibited a significantly ($p < 0.001$) higher mean cloacal temperature (41.32 ± 0.218 ºC) compared to flock C (40.48 ± 0.65 ºC), which were unaffected controls. The average hematological results indicated leukocytosis, heterophilia, lymphopenia, and monocytosis in flock A (**Table 3**). Flock A showed a significantly higher number of leukocytes ($p < 0.001$) and a greater percentage of heterophils ($p = 0.001$), along with a lower percentage of lymphocytes ($p = 0.001$) compared to flock C. Additionally, the absolute leukocyte counts revealed higher number of heterophils ($p = 0.008$) and monocytes ($p = 0.007$) in flock A relative to flock C (**Table 4**). The remaining hematological values were within the RI.

Gross Examination

Macroscopically, the first stage of IDS (T0) was characterized by a thickening (0.5-0.6 cm) and pallor of the intestinal wall, extending from the proximal portion of the jejunum to Meckel´s diverticulum (10-20 cm in length) (**Figs. 1a, b**). The blood vessels of the jejunal mesothelium were prominently dilated. Other consistent findings included a markedly dilated and flaccid proventriculus and atrophic ovarian follicles. In the second stage (T1), the jejunum exhibited severe dilatation, measuring up to 3-5 cm in diameter (**Fig. 1c**). During the third stage (T2), the dilated jejunum was twisted with severe, focal congestion and hemorrhages (10-15 cm in length) (**Fig. 1d**). At sectioning, hemorrhagic contents were observed in the lumen. In all three stages, the wall of the duodenal loop was moderately thickened (0.3-0.6 cm in diameter). No macroscopic changes were observed in the remaining organs.

Histological Examination

In all three stages, the duodenum exhibited moderate lymphoplasmacytic duodenitis, characterized by an increased lymphocytes and plasma cells within the lamina propria, with occasional moderate numbers of heterophils (**Fig. 2a**). The duodenum preserved the villous-to-crypt length ratio, and Lieberkühn's crypts were hyperplastic.

In the first stage (T0), the intestinal villi of affected jejunum had moderate villous blunting (**Fig. 2b**). The villus-to-crypt length ratio ranged from 1:4 to 1:2. Goblet cell hyperplasia was also observed. The intestinal crypts were markedly dilated, and their epithelial cells were hyperplastic. The lamina propria was expanded due to an inflammatory infiltrate primarily composed of heterophils, with fewer lymphocytes and plasma cells.

In the second stage (T1), the intestinal villi of the affected jejunum were atrophied (**Fig. 2c**). Multifocal to coalescent areas of necrosis affected up to 60-70% of the intestinal mucosa, primarily targeting the villus enterocytes and crypts. Remaining crypts displayed epithelial hyperplasia and dilatation, with cell debris present in the lumen. The inflammatory infiltrate extended from the lamina propria into the submucosa, muscularis, and serosal layers, evolving from a predominantly heterophilic component to a mixed population of heterophils and lymphocytes, finally resulting in a lymphoplasmacytic infiltrate. Myenteric and submucosal plexuses, along with ganglia of the subserosa, were infiltrated by lymphocytes and plasma cells, with occasional necrosis of neurons and mineralization (**Figs. 2e, f**). Blood vessels in the serosa were occasionally surrounded by this inflammatory infiltrate. The ventriculus contained multiple ulcers in the mucosa, disrupting the koilin layer and replacing it with cellular debris and bacilli colonies. The lamina propria of ventriculus was expanded by an inflammatory infiltrate primarily composed of degenerated and viable heterophils.

In the third stage (T2), the apical mucosa and crypts of the affected jejunum were 100% necrotic, characterized by a significant amount of cell debris, colonies of bacilli, and extensive hyperemia and hemorrhages (**Fig. 2d**). The lamina propria, muscularis, and serosal layers were diffusely infiltrated by heterophils, lymphocytes, plasma cells, and fewer macrophages. No other histopathological findings were detected in the remaining organs.

Viral and Bacterial Metagenomics

Sampled A1 and A2 hens were diagnosed at the end of stage 1. Viral and bacterial specific read counts, absolute (compared to the total sequenced genome) and relative abundances (%) of families, genera, and species of different layers are summarized in **Supplemental Tables S1** and **S2** and represented in **Supplemental Figures S2 and S3**. Megrivirus was detected in both hens affected by IDS (A1 and A2) (**Supplemental Figure S2**). The megrivirus sequences (PQ468424) corresponded to a fragment of the polyprotein gene of megrivirus, exhibiting 92 % of identity with other megriviruses C1 (MW054511.1, MW054510.1, MW054509.1, MW054505.1). Moreover, relative abundances of *Fusobacterium mortiferum* and *Megamonas funiformis* increased in both affected layers A1 and A2 (**Supplemental Figure S3**).

Discussion

Three sequential stages were identified in commercial brown layers affected with IDS, based on clinicopathological course of the disease. Metagenomic analysis revealed the presence of megrivirus C in the proventriculus and jejunum of affected hens, alongside a significant shift in the gut microbiota. *Fusobacterium mortiferum* and *Megamonas funiformis* were the most abundant bacterial species in proventriculus and jejunum of affected animals.

The subclinical nature of the initial stage IDS-affected hens makes the early detection of this disease challenging. However, as noted in previous studies, the second stage of the disease is marked by significant weight loss, pale and atrophied combs and wattles, and progressive decline in egg production. [22,33] The third stage is characterized by hyperacute mortality caused by large jejunal torsion and vascular involvement, leading to hypovolemic and septicemic shock. In this study, hens from flock A, affected by IDS, exhibited a 0.9 ºC increase in the average cloacal temperature compared to flock C (control). Hematology results also indicated that flock A exhibited a severe heterophilia compared to the control group. These findings suggest that IDS is characterized by a heterophilic inflammatory response, contrary to previous studies that associated IDS with eosinophilic inflammation. [33] Additionally, anemia was not observed in affected animals. Therefore, the observed clinical signs, elevated cloacal temperature, and heterophilia in hematological analysis could contribute to the early diagnosis of IDS.

The lesion progression observed in this study provides further insight into the stages of IDS. The first stage was characterized by proventricular dilatation and thickening of the duodenum and jejunum due to heterophilic and lymphoplasmacytic enteritis. Although these pathological findings have been previously described, the significant jejunal dilatation was not present in the first stage. [22,30,33] Three to five weeks later, in the second stage, intestinal dilatation from the proximal portion of the jejunum to Meckel´s diverticulum was observed, characterized by necrotizing-ulcerative jejunitis. Moreover, heterophilic and lymphoplasmacytic ganglioneuritis, occasional necrosis and mineralization of the myenteric and submucosal plexuses, as well as subserosal ganglia, were identified in the jejunum. Although perineuritis has been associated with the IDS, this study is the first to report ganglioneuritis and mineralization of nervous jejunal plexuses and subserosal ganglia in IDS-affected hens. [22] Neuronal damage was observed

exclusively in hens at the second stage, characterized by severe necrotizing-ulcerative jejunitis. Therefore, we hypothesize that the severe transmural inflammatory infiltrate extends to the nervous plexuses and subserosal ganglia, inducing ganglioneuritis, which chronically progresses to neuronal necrosis and mineralization. This process ultimately leads to neuronal dysfunction, thereby contributing to the intestinal dilatation observed in the affected jejunal segment. Identifying the pathogen responsible for IDS would likely help clarify the origin of this lesion. Unlike prior studies, no lesions were observed in the ileum or pancreas. [22] Seven to eight weeks later, the third stage was characterized by severe jejunal torsion and congestion with hemorrhages. In cases of intestinal torsion, venous return is compromised, leading to a circulatory disorder known as congestion or acute passive hyperemia, which is subsequently followed by hemorrhages. These intestinal torsions were observed exclusively in cases of severe jejunal dilatation, suggesting that torsion may be a secondary lesion. The incidence of intestinal torsions increased following the generalized application of tylosin on the farm (data not shown). It is plausible that prior intestinal dilatation predisposes the intestines to torsion when motility increases due to tylosin administration. In the third stage, ventricular erosions and ulcers were observed. Ventricular ulcers, however, have been associated with various etiologies, including stress and anorexia. [2,8,21] Therefore, ventricular erosions and ulcers are likely secondary to intestinal damage and the marked reduction in water and feed consumption in affected animals. In this study, the reproductive tract was not microscopically studied in the different stages of the disease. Further studies are needed to define the atrophic lesions in the reproductive tract of IDS-affected hens.

IDS has been described in layers and breeders from cage-free farms. [22,30,33] In this study, hens from enriched-cage systems were also affected by IDS, although morbidity appeared lower than in floor-reared systems (data not shown). The global increase in IDS

prevalence may be attributed to the rise in floor-reared poultry systems, probably due to the promotion of fecal-oral transmission of the pathogens involved in this syndrome. Additionally, multiple genetic lines of layers and breeders have been affected, ruling out a genetic association. [22,25,30,33] Based on the clinicopathological and epidemiological findings, an infectious etiology is suggested.

The etiology of IDS has been widely debated, with several potential causative agents considered, including viral infections. [22,30,33] Recently, ChPV and megrivirus have been associated with this syndrome. [22] However, in this study, parvovirus was not detected by metagenomic analysis. Interestingly, a megrivirus, closely related to megrivirus C, was detected in the proventriculus and jejunum of IDS-affected hens but was absent in healthy birds. This contrasts with previous studies that identified megrivirus in the intestinal tracts of healthy chickens. [16,17] IDS is a chronic disease with clinical signs manifesting at 30-40 weeks of age; thus, the detection of megrivirus in the gastrointestinal tract of younger birds does not rule out its pathogenic potential in poultry. Furthermore, megriviruses have been detected in turkeys affected with avian encephalomyelitis, hepatitis, and enteritis and chickens with malabsorption syndrome, runting-stunting syndrome, and necrotizing proventriculitis. [3,5,9,12,13,15,18,20] Therefore, megrivirus could trigger proventricular and intestinal inflammation and immune responses, disrupt the gut microbiota, and synergize with other intestinal bacteria to induce more severe forms of IDS, as seen in later stages. [1,26,27] It should be noted that due to the low depth of the reads, less prevalent viruses, although perhaps contributing to the pathogenesis, may not have been detected by metagenomics. Interestingly, in this study, a marked increase in the abundance of *Fusobacterium mortiferum* and *Megamonas funiformis* was observed in IDS-affected hens compared to healthy animals. In poultry, *F. mortiferum* and *M. funiformis* are anaerobic, gram-negative bacteria that are part of the complex microbial community

inhabiting the gastrointestinal tract. [14,19,24,28] However, under certain conditions, such as stress, immune suppression, or gut dysbiosis, these bacteria may become opportunistic and contribute to disease states. [10]

Megriviruses are highly prevalent in wild birds, turkeys, and free-range poultry. [4,7,29,32] Although most strains are host-specific, the *Megrivirus* genus has a high genetic recombination rate. [3,4,6] Therefore, contact between infected wild birds and free-range hens could play a significant role in the epidemiology of IDS. [4,13,29,31]

In summary, this study provides a detailed description of the clinicopathological progression of IDS in commercial brown layers. Further research is necessary to determine the age at which IDS onset occurs and the duration of each stage. megrivirus C might play a role in triggering or exacerbating the gastrointestinal abnormalities associated with IDS, potentially in conjunction with other opportunistic intestinal bacteria. However, the detection of megrivirus only in two IDS-affected hens is not enough to determine this virus as the causative agent of IDS. Future research should aim to elucidate the pathogenesis of megrivirus in the gastrointestinal system and explore potential coinfections that may contribute to the development of IDS.

Acknowledgments

We are grateful to Álex Cobos from the Centro de Investigación en Sanidad Animal (IRTA-CReSA) and Luis Monteagudo from the University of Zaragoza for their assistance in the interpretation of the pathological and genetic results.

Declaration of Conflicting Interests

The authors declared no potential conflicts of interest with respect to the research, authorship, and/or publication of this article.

Funding

The authors received no financial support for the research, authorship, and/or publication of this article.

Author´s contributions

AG, ARL and DG designed and performed the experiments; EP, SGF and LL contributed to the experimental design; AG, ARL, EP and LL performed the histologic evaluations; AG and DG performed the metagenomic analysis interpretation and the statistical analysis; the manuscript was written by AG and DG with contribution from the other authors.

References

1. Abaidullah M, Peng S, Kamran, et al. Current Findings on Gut Microbiota Mediated Immune Modulation against Viral Diseases in Chicken. Viruses. 2019;11(8).

2. Abdul-Aziz T, Fletcher OJ, Barnes HJ, et al. Avian histopathology: 4th Edition; 2016.

3. Boros Á, Pankovics P, Adonyi Á, et al. Genome characterization of a novel chicken picornavirus distantly related to the members of genus Avihepatovirus with a single 2A protein and a megrivirus-like 3′ UTR. Infect Genet Evol. 2014;28:333–338.

4. Boros Á, Pankovics P, Knowles NJ, et al. Comparative Complete Genome Analysis of Chicken and Turkey Megriviruses (Family Picornaviridae): Long 3′ Untranslated Regions with a Potential Second Open Reading Frame and Evidence for Possible Recombination. J Virol. 2014;88(11):6434–6443.

5. Devaney R, Trudgett J, Trudgett A, et al. A metagenomic comparison of endemic viruses from broiler chickens with runting-stunting syndrome and from normal birds. Avian Pathol.2016;45(6):616–629.

6. Farkas T, Fey B, Hargitt E, et al. Molecular detection of novel picornaviruses in chickens and turkeys. Virus Genes. 2012;44(2):262.

7. Fu H, Chen S, Zhang J, et al. Rapid detection of goose megrivirus using TaqMan real-time PCR technology. Poult Sci. 2024;103(5):103611.

8. Gjevre AG, Kaldhusdal M, Eriksen GS. Gizzard erosion and ulceration syndrome in chickens and turkeys: a review of causal or predisposing factors. Avian Pathol. 2013;42(4):297–303.

9. Honkavuori KS, Shivaprasad HL, Briese T, et al. Novel picornavirus in Turkey poults with hepatitis, California, USA. Emerg Infect Dis. 2011;17(3):480–487.

10. Jing Z, Zheng W, Jianwen S, et al. Gut microbes on the risk of advanced adenomas. BMC Microbiol. 2024;24(1):1–14.

11. Kapgate SS, Kumanan K, Vijayarani K, et al. Avian parvovirus: classification, phylogeny, pathogenesis and diagnosis. Avian Pathol. 2018;47(6):536–545.

12. Kim HR, Kwon YK, Jang I, et al. Viral metagenomic analysis of chickens with runting-stunting syndrome in the Republic of Korea. Virol J. 2020;17(1):1–10.

13. Kim HR, Yoon SJ, Lee HS, et al. Identification of a picornavirus from chickens with transmissible viral proventriculitis using metagenomic analysis. Arch Virol. 2015;160(3):701–709.

14. Kollarcikova M, Kubasova T, Karasova D, et al. Use of 16S rRNA gene sequencing for prediction of new opportunistic pathogens in chicken ileal and cecal microbiota. Poult Sci. 2019;98(6):2347–2353.

15. Kubacki J, Qi W, Fraefel C. Differential Viral Genome Diversity of Healthy and RSS-Affected Broiler Flocks. Microorganisms. 2022;10(6):1092.

16. Kwok KTT, Rooij MMT de, Messink AB, et al. Genome Sequences of Seven Megrivirus Strains from Chickens in The Netherlands. Microbiol Resour Announc. 2020;9(47).

17. Lima DA, Cibulski SP, Finkler F, et al. Faecal virome of healthy chickens reveals a large diversity of the eukaryote viral community, including novel circular ssDNA viruses. J Gen Virol. 2017;98(4):690–703.

18. Lima DA, Cibulski SP, Tochetto C, et al. The intestinal virome of malabsorption syndrome-affected and unaffected broilers through shotgun metagenomics. Virus Res. 2019;261:9–20.

19. Liu X, Wang C, Wang Y, et al. Age-associated changes in the growth development of abdominal fat and their correlations with cecal gut microbiota in broiler chickens. Poult Sci. 2023;102(9):102900.

20. Marvil P, Knowles NJ, Mockett APA, Britton P, Brown TDK, Cavanagh D. Avian encephalomyelitis virus is a picornavirus and is most closely related to hepatitis A virus. J Gen Virol. 1999;80 (Pt 3)(3):653–662.

21. Mirzazadeh A, Asasi K, Schachner A, et al. Gizzard Erosion Associated with Fowl Adenovirus Infection in Slaughtered Broiler Chickens in Iran. Avian Dis. 2019;63(4):568–576.

22. Nuñez LFN, Chacón RD, Charlys da Costa A, et al. Detection and molecular characterization of chicken parvovirus and chicken megrivirus in layer breeders affected by intestinal dilatation syndrome. Avian Patho. 2024; 53(6):520-532.

23. Nuñez LFN, Santander-Parra SH, De la Torre DI, et al. Molecular Characterization and Pathogenicity of Chicken Parvovirus (ChPV) in Specific Pathogen-Free Chicks Infected Experimentally. Pathogens. 2020;9(8):1–14.

24. Oakley BB, Lillehoj HS, Kogut MH, et al. The chicken gastrointestinal microbiome. FEMS Microbiol Lett. 2014;360(2):100–112.

25. Perez S. Intestinal dilatation in layers. Vet Rec. 2005;157(4):123–124.

26. Quinteiro-Filho WM, Gomes AVS, Pinheiro ML, et al. Heat stress impairs performance and induces intestinal inflammation in broiler chickens infected with Salmonella Enteritidis. Avian Pathol. 2012;41(5):421–427.

27. Quinteiro-Filho WM, Ribeiro A, Ferraz-de-Paula V, et al. Heat stress impairs performance parameters, induces intestinal injury, and decreases macrophage activity in broiler chickens. Poult Sci. 2010;89(9):1905–1914.

28. Roth C, Sims T, Rodehutscord M, et al. The active core microbiota of two high-yielding laying hen breeds fed with different levels of calcium and phosphorus. Front Physiol. 2022;13:951350.

29. Shan T, Yang S, Wang H, et al. Virome in the cloaca of wild and breeding birds revealed a diversity of significant viruses. Microbiome. 2022;10(1):1–21.

30. Twomey DF, Wood AM, Young SCL. Intestinal dilatation in organic layers. Vet Rec. 2005;157(2):63–64.

31. Vibin J, Chamings A, Klaassen M, et al. Metagenomic characterisation of avian parvoviruses and picornaviruses from Australian wild ducks. Sci Rep. 2020;10(1):1–15.

32. Wille M, Eden JS, Shi M, et al. Virus–virus interactions and host ecology are associated with RNA virome structure in wild birds. Mol Ecol. 2018;27(24):5263.

33. Zavala, G., Williams, S. M., et al. Clinical presentation and pathology of intestinal dilatation syndrome (IDS) in cage-free brown layer breeders and brown layers. 2013. Presented at: 2013 AAAP. AVMA Annual Meeting.

Tables

Table 1. Major clinical signs, gross and histopathological findings useful to differentiate between the three sequential stages of intestinal dilation syndrome (IDS). The features are arranged in order of importance for the diagnosis of IDS.

	Clinical signs	Gross lesions	Histopathology
First stage (T0) **(n=6)**	Subclinical (n=6)	Proventricular dilation (n=6) Duodenal thickening (n=6) Jejunal thickening (n=6) Ovarian follicular atrophy (n=6)	Heterophilic and lymphoplasmacytic jejunitis (n=6) Lymphoplasmacytic duodenitis (n=6)
Second stage (T1) **(n=13)**	Cachexia (n=9) Pale and small comb and wattles (n=13) Egg drop (n=13) Cessation of laying (n=13) "Poulet chirp" (n=13)	Jejunal dilation (n=13) Proventricular dilation (n=13) Duodenal thickening (n=13) Ovarian follicular atrophy (n=13)	Necrotic, lymphoplasmacytic and heterophilic jejunitis (n=13) Jejunum: lymphoplasmacytic ganglioneuritis (n=9) Jejunum: mineralization of nervous plexuses and subserosal ganglia (n=6) Lymphoplasmacytic duodenitis (n=13)
Third stage (T2) **(n=6)**	Hyperacute mortality (n=6)	Jejunal torsion-volvulus (n=6) Jejunal acute passive hyperemia (n=6) Jejunal hemorrhages (n=6)	Necrotic and haemorrhagic jejunitis (n=6) Lymphoplasmacytic duodenitis (n=6)

Abbreviations: T0: day 0; T1: Three to five weeks after the first sampling; T3: two to three weeks after the second sampling

Table 2. Percentage of animals from the three flocks at different sequential stages of intestinal dilation syndrome.

	First stage (T0)	Second stage (T1)	Third stage (T3)
Flock A (n = 20)	20% (n=4)	50% (n=10)	30% (n=6)
Flock B (n = 5)	33% (n=2)	67% (n=3)	0%
Flock C (n =10)	0%	0%	0%

Abbreviations: T0: day 0; T1: Three to five weeks after the first sampling; T3: two to three weeks after the second sampling

Table 3. Blood count differences between healthy and intestinal dilation syndrome affected commercial brown layers in stage 2.

		Hematocrit (L/L)	Hemoglobin (g/L)	Leukocytes (g/L)*	Heterophils (%)*	Lymphocytes (%)*	Monocytes (%)	Eosinophils (%)	Basophils (%)
Flock C (n = 5)	Mean	0.31	71.8	14.05	44.8	45.6	9	0.4	0.2
	SD	0	2.48	1.63	5.2	5.76	3.08	0.25	0.2
Flock A (n = 5)	Mean	0.33	74	40.22	71.8	14.6	15	1.2	0.4
	SD	0.21	6	2.42	2.22	2.8	3.91	1.2	0.23

Note: Statistically significant differences between groups (*p < 0.05).
SD: standard deviation.

Table 4. Absolute values of leukocytes in blood count differences between healthy and intestinal dilation syndrome affected commercial brown layers in stage 2.

		Heterophils (g/L)*	Lymphocytes (g/L)	Monocytes (g/L) φ	Eosinophils (g/L)	Basophils (g/L)
Flock C (n = 5)	Mean	6.5	6.32	1.18	0.04	0.02
	SD	1.49	0.87	0.31	0.24	0.02
Flock A (n = 5)	Mean	29	5.8	5.9	0.46	0.18
	SD	2.47	1.09	1.27	0.46	0.11

Note: Statistically significant differences between groups (*p < 0.05; φp < 0.05).
SD: standard deviation.

Figure legends

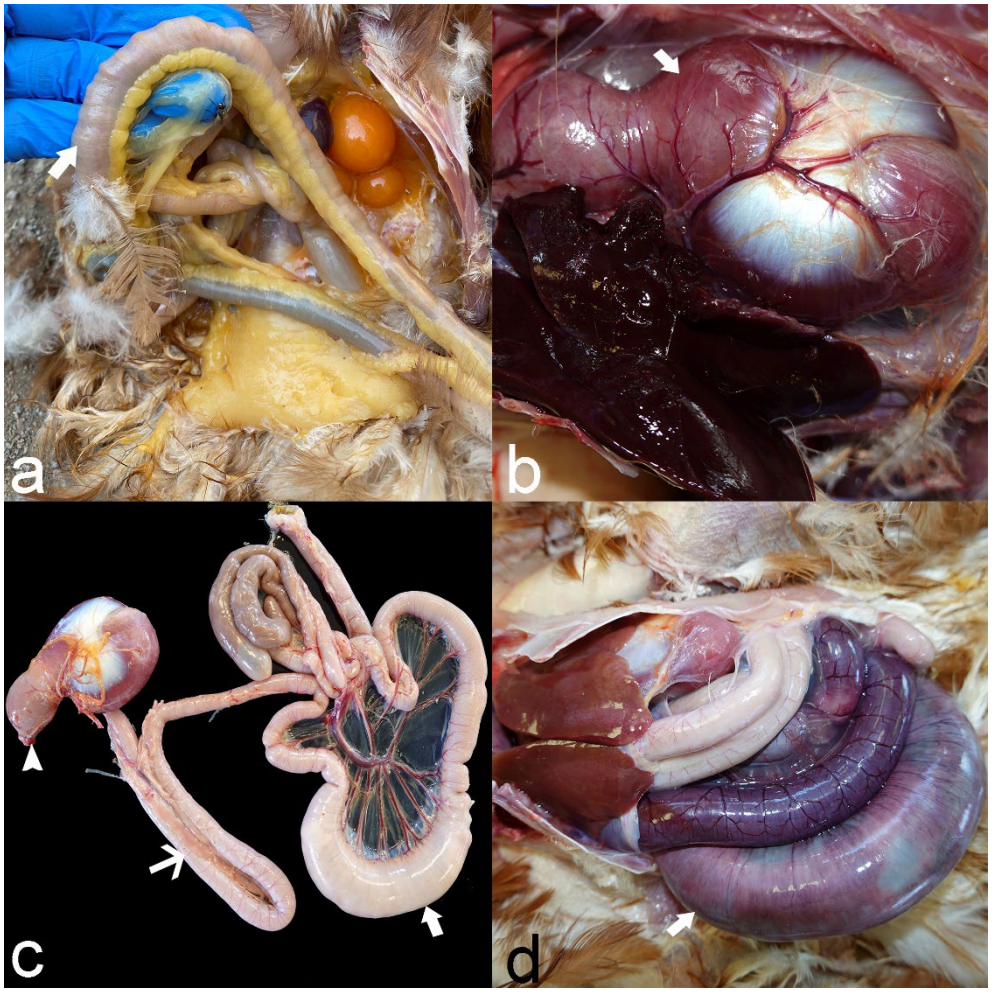

Figure 1. Intestinal dilatation syndrome in 50-week-old, commercial brown laying hens. **a)** First stage. The intestinal wall of the jejunum is thickened (arrow). **b)** First stage. The proventriculus is dilated showing an hourglass shape (arrow). **c)** Second stage. The proventriculus is dilated (arrowhead), the duodenal loop is thickened (thin arrow) and the jejunum, from the proximal portion to the Meckel´s diverticulum, is dilated up to 2.5 cm (thick arrow). **d)** Third stage. Jejunal acute passive hyperemia with hemorrhages (arrow) resulting from torsion of the dilated part of the jejunum.

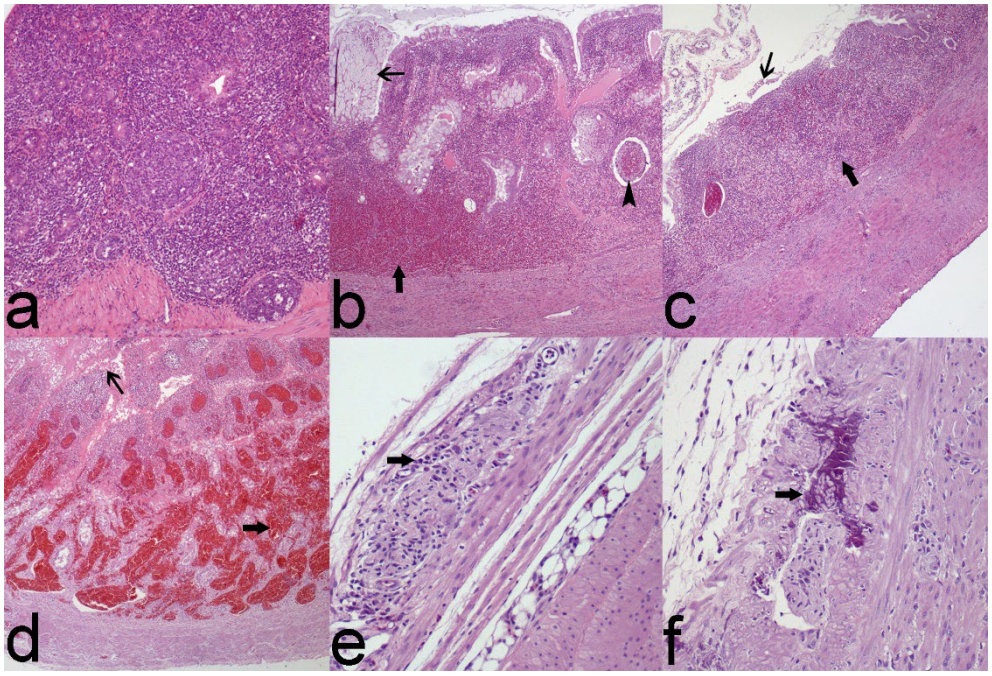

Figure 2. Intestinal dilatation syndrome in 50-week-old, commercial brown laying hens. Hematoxylin and eosin. **a)** First stage, duodenum. The lamina propria is densely and diffusely infiltrated by lymphocytes and plasma cells. **b)** First stage, jejunum. Villi are shortened, thickened, and fused. The lamina propria is infiltrated by numerous heterophils (arrow) and lesser numbers of lymphocytes and plasma cells. Goblet cells are hyperplastic (thin arrow), and crypts are dilated with cell debris in their lumen (arrowhead). **c)** Second stage, jejunum. Epithelium is lost, and villi are atrophic and fused (thin arrow). The lamina propria is infiltrated by a mixture of lymphocytes, plasma cells, and heterophils (arrow). Inflammatory cells extend into the submucosa, muscular layer, and serosa. **d)** Third stage. The jejunal mucosa is nearly 100% necrotic (thin arrow) and is replaced by degenerated heterophils and lymphocytes. In the lamina propria, there is severe hyperemia along with hemorrhages (arrow). **e)** Second stage. Ganglia of the subserosa are infiltrated by lymphocytes and plasma cells (arrow). **f)** Third stage. Mineralization of subserosal ganglia is evident.